

and that in the dense phase. The former factor is more significant when  $U_{mf}$  is larger. Both these factors would tend to reduce backmixing in beds fitted with horizontal tubes. In addition, it is known from the work of Botterill et al. (1970) that fluidized solids flowing horizontally through tube banks encounter considerable resistance to flow. A rough estimate based on that work suggests a pressure differential of 100 mm W.G. would be required to move sand S1 at a velocity of  $0.2 \text{ m s}^{-1}$  through the tube bundle employed. By comparison, the pressure differential in an open (that is, no tubes) bed is about 30 mm W.G. (Whitehead et al., 1977). Thus, a reduction in solids circulation because of flow resistance must also play a large part.

#### LITERATURE CITED

- Botterill, J. S. M., R. Chandrasekhar and M. Van der Kalk, "Heat Transfer and Pressure Loss in the Flow of Fluidized Solid Across Banks of Tubes," *Brit. Chem. Eng.*, **15**, 769 (1970).
- Harrison, D., and J. R. Grace, *Fluidization*, J. F. Davidson and D. Harrison, ed., Chapt. 13, Academic Press, New York (1971).
- Hamilton, C. J., C. Fryer and O. E. Potter, "Back-mixing of Gas in Fluidized Beds," *Chemeca '70*, Session I, Inst. Chem. Engrs., London, England (1970).
- Latham, R., and O. E. Potter, "Backmixing of Gas in a 6-in Diameter Fluidized Bed," *Chem. Eng. J.*, **1**, 152-161 (1970).
- Newby, R. A., and D. L. Keairns, "Fluidized Bed Heat Transport Between Parallel Horizontal Tube-Bundles," *Proceedings of the Second Engineering Foundation Conference on Fluidization*, Eds. J. F. Davidson and D. L. Keairns, ed., p. 320, Cambridge Univ. Press, England (1978).
- Nguyen, H. V., A. B. Whitehead and O. E. Potter, "Gas Backmixing, Solids Movement and Bubble Activities in Large-Scale Fluidized Beds," *AIChE J.*, **23**, 913 (1977).
- Nguyen, H. V., A. B. Whitehead and O. E. Potter, "Gas Backmixing in Large Fluidized Beds," *Proceedings of the Second Engineering Foundation Conference on Fluidization*, J. F. Davidson and D. L. Keairns, ed., p. 387, Cambridge Univ. Press, England (1978).
- Nguyen, H. V., A. B. Whitehead and O. E. Potter, "Bubble Distribution and Eruption Diameter in Fluidized Beds with Horizontal Tube Bundles," *Chem. Eng. Sci.*, **34**, 1163-1164 (1979).
- Nguyen, H. V., and O. E. Potter, "Adsorption Effects in Fluidized Beds," in *Fluidization Technology*, Dale L. Keairns, ed., vol. II, p. 183, McGraw Hill, New York (1975).
- Whitehead, A. B., G. Gartside and D. C. Dent, "Flow and Pressure Maldistribution at the Distributor Level of a Gas-Solid Fluidized Bed," *Chem. Eng. J.*, **1**, 175 (1970).
- Whitehead, A. B., D. C. Dent and J. C. M. McAdam, "Fluidization Studies in Large Gas-Solid Systems, Part V, Long and Short Term Pressure Instabilities," *Powder Tech.*, **18**, 231 (1977).
- Xavier, A. M., D. A. Lewis and J. F. Davidson, "The Expansion of Bubbling Fluidized Beds," *Trans. I. Chem. E.*, **56**, 274 (1978).

Manuscript received February 12, and accepted February 29, 1980.

## "Fine Structure" of the CSTR Parameter Space

D. C. WILLIAMS and J. M. CALO

Dept. of Chemical Engineering  
Princeton University  
Princeton, N.J. 08544

In a now classic paper, Uppal, Ray, and Poore (1974) (herein after referred to as URP) reported on an exhaustive study of the dynamic behavior of the continuous stirred tank reactor with a single, first-order, irreversible, exothermic reaction. The results were conveniently summarized using phase plane plots and parameter space maps. During the course of our own research, we have had occasion to refer to this work. This led us to discover some additional, and as yet unreported, subdivisions of the parameter space which yield new qualitative behavior, hence the purpose of this note.

For brevity, we refer the reader to the referenced paper and assume the same notation. Although URP thoroughly investigated the parameter space boundaries created by the coincidence of the roots  $s_1$ ,  $s_2$ ,  $m_1$ , and  $m_2$  in the conversion coordinate,  $x_{1s}$  (i.e., curve SM), they overlooked the demarcations created by the coincidence of the Damkohler numbers corresponding to these roots. In Figure 1, which is not drawn to scale in order to show all regions clearly, we present our proposed additions to the original parameter space plot (i.e., Figure 5 of URP) created by equating the Damkohler numbers corresponding to the various roots.

As can be seen, two additional boundaries result—SMDa and SSDa. SMDa separates regions IVa and IVb, which although reported by URP as having qualitatively different behavior, were not separated by an analytical boundary. SMDa also gives rise to several new regions by dividing region VI into VIa, and VIb, and VIc; region IIIb into IIIb and IIIc; and also separates region IVa from IVd. SSDa subdivides region IV into IVc and IVd. Figure 2 shows these regions to scale. The lines SMDa and SSDa are so close that they cannot be distinguished clearly. The

difference in the  $B$  values on these curves is 0.00003 for  $1+\beta=5$  and 0.03 for  $1+\beta=10$ .

SMDa is found by solving for  $B$  and  $1+\beta$  such that  $Da(s_{1,2}) = Da(m_{1,2})$ . In particular:  $Da(s_1) = Da(m_2)$  along the line segment emanating from point  $P$  to the right;  $Da(s_1) = Da(m_1)$  along the line segment  $PQ$ ; and  $Da(s_2) = Da(m_1)$  along the remainder. No corresponding  $Da(s_2) = Da(m_2)$  exists other than the one already determined by SM since  $s_2 > m_1$ . SSDa is found by solving  $Da(s_1) = Da(s_2)$ . SSDa is not extended beyond point  $R$  because in region III  $m_1 < s_1 < m_2 < s_2$ ; therefore, the condition  $Da(s_1) = Da(s_2)$  demarcates no new behavior. Note that all the resultant equations are transcendental but are easily solved by Newton-Raphson techniques, for example.

The corresponding conversion vs.  $Da$  plots for the new regions are presented in Figure 3. All labeling corresponds to the original notation of URP with the original region VI corresponding to the new region VIb of Figure 3. The qualitative behavior of the new regions is discussed below.

#### REGION III

The new region is IIIc, which differs from IIIb in that the  $Da$  at which bifurcation to the stable limit cycle occurs is less than the maximum  $Da$  at which multiplicity occurs. This leads to the different qualitative behavior shown in Figure 3, wherein the "B"-type phase plane behavior of IIIb is supplanted by the "E"-type behavior of region IIIc for the designated portion of region III, or equivalently, the "H"-type behavior of region IIIa is supplanted by the "F"-type behavior of region IIIc. This leads to a previously unreported hysteresis behavior.

For large  $Da$ , there exists a unique, high conversion stable steady state. As  $Da$  is decreased, this steady state destabilizes

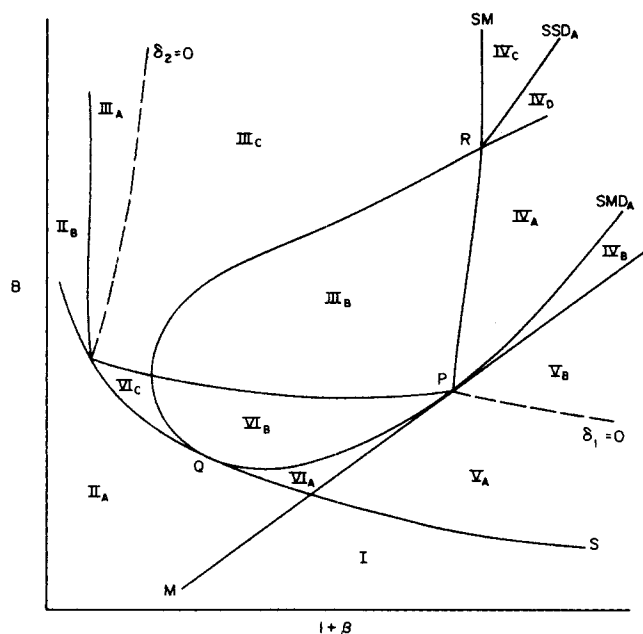


Figure 1. Qualitative classification of dynamic behavior in parameter space.

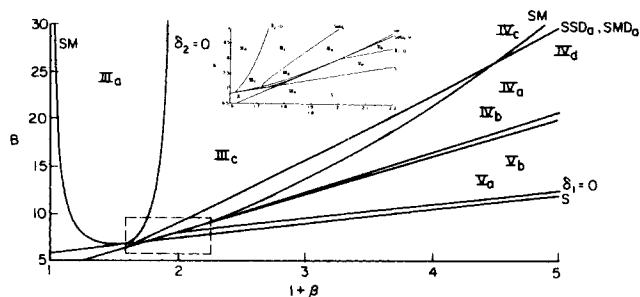


Figure 2. Classification of dynamic behavior in parameter space ( $\gamma \rightarrow \infty$ ,  $x_{2c} = 0$ ) to scale.

and a stable limit cycle bifurcates to the left and grows steadily, until it coalesces with a separatrix and disappears, leaving the system in a unique, low conversion steady state. This behavior is the same as reported by URP for region IIIb. However, if now  $Da$  is increased, the reactor remains in the stable, low conversion steady state and then jumps directly to the stable, high conversion steady state without proceeding through the stable limit cycle.

#### REGION IV

The new regions are IVc and IVd, which differ from IVa in much the same manner that IIIc differs from IIIb; i.e., bifurcation of the stable limit cycle occurs at a  $Da$  less than the maximum  $Da$  at which multiplicity occurs. As for region IIIc, the stable limit cycle would not be observed if  $Da$  were increased slowly from a low value in either region IVc or IVd. IVc and IVd differ from each other in that IVc exhibits a region with an unstable limit cycle encircling the stable, low conversion steady state (type "H"), while the corresponding phase plane behavior in IVd is that of a stable limit cycle encircling the unstable, high conversion steady state (type "G").

It is also noted that two types of conversion vs.  $Da$  plots have been found in region IVa: the type shown in Figure 4a, and the type shown in Figure 4b. It was decided not to label these as separate subregions for both experimental and computational reasons. The regions could only be distinguished via transient experiments as opposed to the steady state type of hysteresis experiment discussed above. Also, the boundary between the two regions is not given by an analytical expression as for the others, but rather must be generated by performing a large

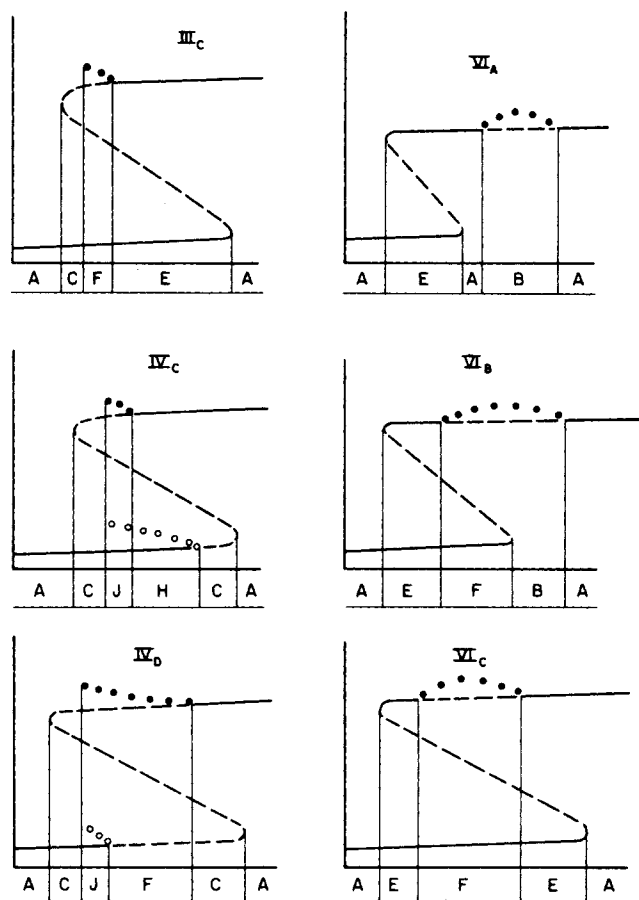


Figure 3. Conversion vs.  $Da$  for new regions.

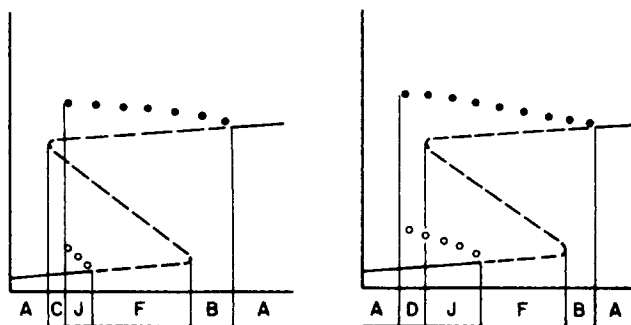


Figure 4. Alternate conversion vs.  $Da$  diagrams for region IVa.

number of integrations of the CSTR equations, which for most practical purposes is prohibitive.

#### REGION VI

Regions VIa, VIb, and VIc can be distinguished by the change in steady state behavior as  $Da$  is increased, from a low value. In VIa, as  $Da$  is increased, the reactor passes from a unique, low conversion, stable steady state to a unique, stable, high conversion steady state, and then to a stable limit cycle which initially grows and then shrinks and returns to a unique, stable, high conversion steady state. In VIb, the reactor jumps directly to the stable limit cycle; thus, the limit cycle bifurcation is not observed. In VIc, the reactor jumps directly from a unique, stable, low conversion steady state to the unique, stable, high conversion steady state; the limit cycle is not observed at all. However, the behavior as  $Da$  is decreased from a high value is the same for all subregions: unique, stable, high conversion steady state, followed by a stable limit cycle which grows and then shrinks, passing back to a stable, high conversion steady state, and finally

## SUMMARY

Several new regions in the CSTR parameter space, defined by additional boundaries, have been defined. The most significant new behavior is a type of hysteresis in which a stable limit cycle can be attained upon decreasing  $Da$  from low values. These additions to the fine structure of the CSTR parameter space once again underscore the richness of the dynamic behavior of this relatively simple model. It must also be noted that the additional subdivisions reported here will have direct analogs in other lumped and distributed parameter systems. One should be

particularly aware of these boundaries when probing parameter space for specific dynamic behavior.

## LITERATURE CITED

Uppal, A., W. H. Ray, and A. B. Poore, "On the Dynamic Behavior of the Continuous Tank Reactor," *Chem. Eng. Sci.*, **29**, 967-985 (1974).

Manuscript received October 12, 1979; revision received March 19, and accepted April 7, 1980.

# Bounds on the Variation of $K$ -Value with Various True Boiling Point Fractions Resulting From the Pseudo-Component Approximation: Application to a $H_2$ -Coal Liquid System

PERVAIZ NASIR

and

RIKI KOBAYASHI

Rice University

Houston, Texas 77001

In  $H_2$ -coal liquid systems, the determination of  $H_2$   $K$ -value is straightforward. However, this is not so for the coal liquid. The reason is that the coal liquid components defy separation, identification, and analysis since for all practical purposes they are represented by an infinite number of components. That is to say, the heavier coal liquids represent *continua* mixtures of infinite number of "continua" components. In general, for vapor liquid equilibrium (*VLE*) measurements and calculations such liquids are divided into short boiling range *cuts*, and each of these *cuts* is identified by an average molecular weight, average boiling point, density, etc.

White and Brown (1942) obtained experimental *VLE* data for petroleum fractions boiling from 308.15K (95°F) to 672.05K (750°F) at temperatures from 422.05 to 710.95K and at pressures from 0.345 to 4.823 MPa. From the results of the equilibrium, flash vaporization runs *VLE* phase distributions were derived for arbitrary hypothetical components having a true boiling point (*TBP*) range of 27.8K (50°F). These 27.8K cuts were converted to moles using average molecular weights and gravities and were used to compute  $K$ -values for each of the cuts.

Grayson and Streed (1963) also used arbitrary cuts of 27.8K (50°F) (except for one cut of 13.9K) in the measurement of *VLE* data of  $H_2$ -gas oil systems up to a temperature 755.35K. These gas-oils were typical of commercial hydrocracker feed stocks.

There is some question as to whether or not experimental  $K$ -values of the heavy liquid *cuts* reported in the literature take into account the differences in the volatility of various components within a given cut. The literature values are reported as *average*  $K$ -values for the entire *TBP cut* and are applied independently of the degree of vaporization achieved within each *cut*.

The objective of this investigation is to assess the effect of various *TBP* widths on the error that could result in the measurement of  $K$ -value of this arbitrary boiling range fraction (or *cuts*). It is shown that such an approach can cause severe inherent errors in the  $K$ -value measurements of the *cuts* and thus

reduce their utility.

## ANALYSIS PROCEDURE

The Grayson and Streed (1963) (*GS*) correlation is used to compute  $K$ -values for several  $H_2$ -*continua* component pseudo binary mixtures. The *GS* correlation is an extension of Chao and Seader (1961) correlation for application up to about 728K. The  $K$ -value is computed from the relation:

$$K = y/x = \frac{v^s \gamma}{\phi}$$

$\phi$  and  $\gamma$  are computed respectively from the Redlich-Kwong equation of state and from Scatchard-Hildebrand (solubility parameter) correlation.  $v^s$  is given by Grayson and Streed as an empirical function of reduced temperature, reduced pressure, and acentric factor. This function was obtained from fitting of their high temperature *VLE* data on  $H_2$ -gas oil systems. These authors have also reported all the necessary parameters (viz. solubility parameter,  $\omega$ ,  $T_c$ ,  $P_c$ , and molar liquid volume) for arbitrary "components" having *TBP* range of 27.8K (50°F) from 338.75 to 644.25K. These parameters were calculated at average boiling point of each 27.8K fraction. For this investigation, these parameters were plotted against *TBP*, and a continuous curve was drawn through these plateaus to obtain "averaged" parameter values along the entire *TBP* range. The point values representing each "continua" component were then read from such a curve for each parameter.

The coal liquid considered for analysis is the blended feed in Exxon-Donor-Solvent (*EDS*) process (Epperly, 1978). This blended feed is represented by the *TBP* curve shown in Figure 1. It was shown (Epperly, 1978) that the *TBP* curves for petroleum and coal liquids are very similar, and hence many of the correlations developed for heavy petroleum fluids can be used to predict the approximate behavior of coal liquids. Frith et al. (1979) have proposed certain empirical adjustments in petroleum correlations for making them more accurate for the prediction of *VLE* in  $H_2$ , light gases, and coal liquid systems. These